

Fig. 17. (continued).

Table 5
Summary of initial stiffness (kN/mm).

Story	Story total	PTF	Frame	SW
1	24.35	10.64	2.15	11.56
2	15.07	7.96	1.89	5.22

than Northridge, observed by the maximum acceleration response. The amplification factors range from 1.93 to 3.58, and the maximum one, 3.58, is in Case 2-7 s with PGA of 0.59 g. A scatter diagram of acceleration amplification factor versus base excitation PGA is plotted in Fig. 14, which includes results of the Northridge and Superstition Hills ground motion cases. Fig. 15 shows the absolute acceleration time history of the test structure in Case 1-8, in which the excitation record's

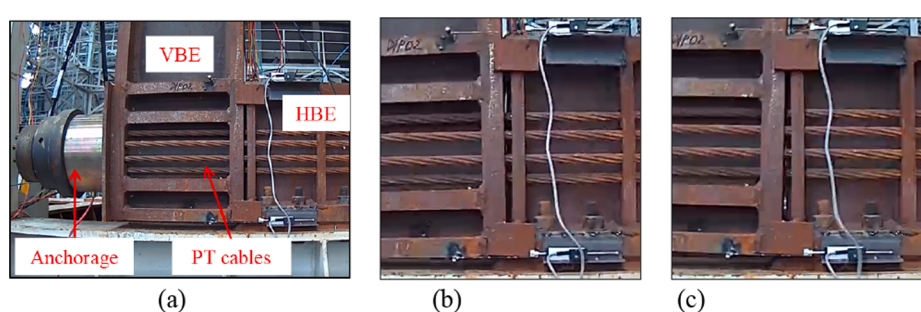


Fig. 18. Photos of PT connection states during test: (a) closed gap; (b) open upper gap; (c) open lower gap.

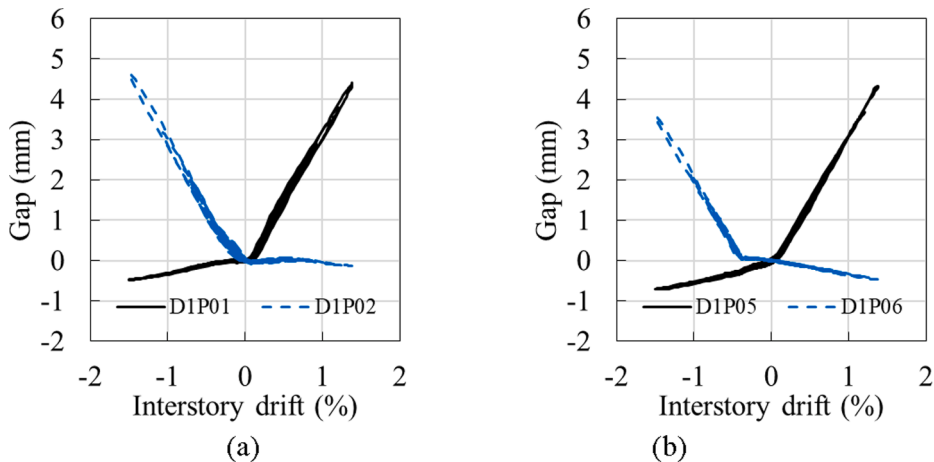


Fig. 19. Gap opening width vs. inter-story drift of 1st-story under Case 1–11 s: (a) bottom in south side; (b) upper in south side.

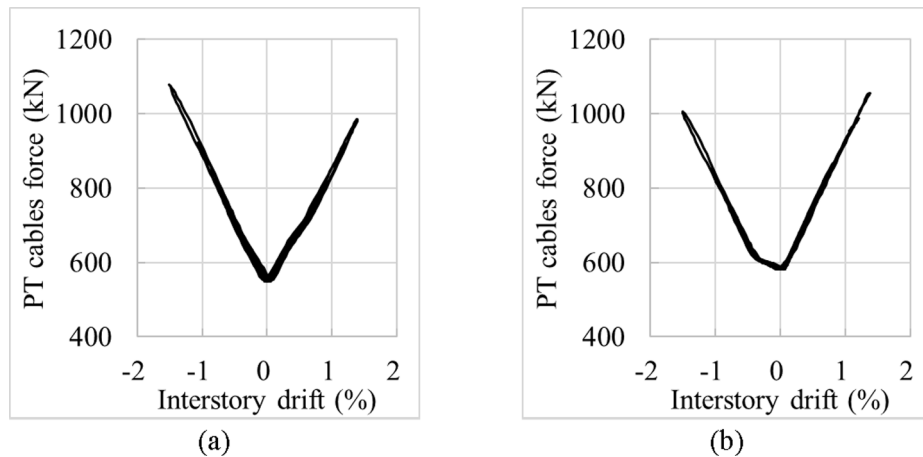


Fig. 20. PT cables force vs. inter-story drift of 1st-story under Case 1–11 s: (a) bottom PT cables; (b) upper PT cables.

PGA value was near the moderate hazard level (0.56 g).

4.4. Displacement response

The peak inter-story drift and residual story drift in each case are listed in Table 4. The peak inter-story drifts are 0.31% and 0.35% in Case 1–4 and Case 2–3 (with PGA of 0.2 g), respectively, which meet the drift limit of 0.4% specified by CSDB (2010) [38].

In Case 1–11 s (Northridge, 1.16 g) and Case 2–7 s (Superstition, 0.59 g), the peak inter-story drifts are 1.61% and 1.40%, respectively. However, the residual inter-story drifts are only 0.013% and 0.017%, which are much less than 0.2% for structure re-centering limit, based on the out-of-plumb tolerances for construction [44]. The test results show that the test structure has such a strong re-centering force that can make the structure return to the pre-earthquake position with the resistance caused by plastic deformation of SWs after a severe earthquake.

By comparing the peak inter-story drifts in Case 1–2, Case 1–13 and Case 1–14 s, it is found that the peak inter-story drifts, as well as the acceleration amplification factors, are very close to each other. Since SWs were replaced before Case 1–13, this verifies that the structural condition of the retrofitted test structure with only damaged SWs being replaced has been restored to pre-earthquake state.

Fig. 16 shows typical inter-story drift ratio (θ) time history curve in Case 1–11 s and Case 2–7 s. As shown in Table 4, the distribution of inter-story drift is quite uniform in all cases (including the cases with relatively high PGA). It can be found that there are fairly small residual

inter-story drifts under any ground motions with different PGA and the test structure can re-center itself.

4.5. Internal force response

The hysteretic behaviors of the test structure in the loading direction are investigated, since the structure was only loaded in the X direction. Two test cases, Case 1–2 and Case 1–11 s, are selected to demonstrate the hysteretic behaviors of the test structure when subjected to Northridge ground motion under two different intensity levels. Fig. 17 shows the hysteresis loops of different stories, SCMPs, PTFs and structural frame in these cases. The story shear force of Story i is obtained as the summation of the total inertia force of upper floors above Story i level. The inertia force of each floor is calculated by multiplying the acceleration with the corresponding floor mass. The story shear force in Fig. 17 has been normalized with the total weight, W , of the test structure ($W = 324.7$ kN). From the hysteretic response presented, the following observations are made:

- (1) As shown in Fig. 17 (a), when the structure is subjected to Northridge with PGA of 0.11 g (Case 1–2), the hysteretic curves show linear behavior, which indicates that the structure remained essentially elastic and did not dissipate much energy through steel yielding. Furthermore, the contribution to lateral resistance from the structural gravity load carrying beam-through frame is relatively small in comparison with the corresponding

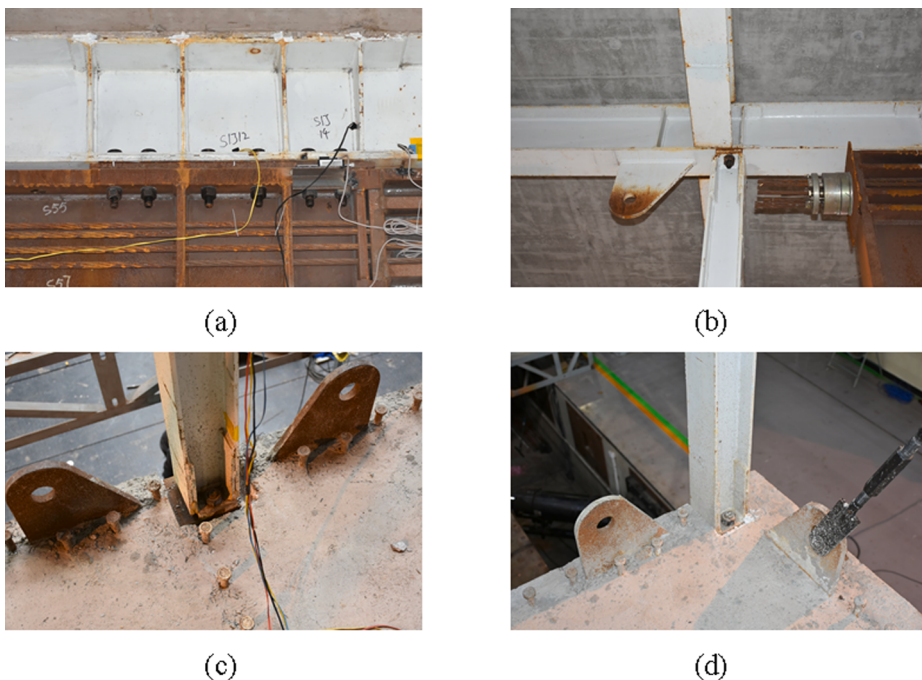


Fig. 21. Photos of test structure after test Case 1-11ss: (a) HBE-to-beam joint; (b) beam-to-column joint near SCMP; (c) middle beam-to-column joint in exterior frame; (d) corner beam-to-column joint.

Table 6
Measured pre-tensioning stress in PT cable groups (unit: MPa).

Case (finishing)	1st-story PTF		2nd-story PTF	
	Lower	Upper	Lower	Upper
Initial state	484.8	516.9	603.2	421.6
1-4	486.5	516.4	610.2	415.5
1-6	486.0	516.7	611.1	415.0
1-8	486.2	518.7	609.5	413.8
1-11 s	489.5	518.3	611.4	411.8
2-3	490.3	519.1	611.4	413.0
2-5	489.9	519.1	608.5	414.4
2-7 s	489.5	519.0	608.8	413.0

story shear. **Table 5** lists the initial elastic stiffness of each structural components derived from measured data. The results show that the gravity load carrying frame's initial stiffness of the two stores are only 8.8% and 12.5% of the story initial stiffness, respectively, and that PTFs and SWs provide the most seismic lateral stiffness of the structure.

- (2) When the test structure is subjected to Northridge earthquake with PGA of 1.16 g (Case 1-11 s), hysteretic behavior of the structure, as shown in **Fig. 17** (b), is clearly different from that of Case 2-1. The story hysteretic curves have flag-shaped behavior, while the structural gravity load carrying frame remain elastic and its hysteresis still presents an elastic linear behavior the same as Case 1-2. The hysteretic curves of PTF show an elastic bilinear behavior. After gap opening in PT connection, the PTF exhibited a reduced stiffness (post-gap-opening stiffness or recentering stiffness) in its elastic bilinear hysteresis loop. The gap opening occurs at inter-story drift of about 0.3% to 0.5%, which is designed to be around 0.4% (the inter-story drift limit of elastic design in CSDB [38]) under frequent ground motions. The gaps would open when the seismic hazard level is greater than frequent ground motions, and after that stiffness of the system decreases to post-gap-opening stiffness. PT connections gap would be closed after unloading because of the large re-centering force from PT cables.

Fig. 18 shows the different states of PT connection during testing, being recorded by a camera attached to the specimen. Additionally, gap opening was measured by corresponding displacement transducers installed between the HBE and VBE at the monitored PT connections. **Fig. 19** shows the gap versus inter-story drift curves of the 1st-story PTF under Case 1-11 s. Clearly, the gap opened and closed as expected during the shake table test. **Fig. 20** shows the PT force versus inter-story drift curve of the 1st-floor under Case 1-11 s. Here it should be noted that the PT force was calculated as the initial PT force plus the increased force due to gap opening and corresponding PT cable elongation.

Once gap opened, the inter-story drift response would increase, which makes the SWs dissipate more energy. It is worth to note that the frame presents an elastic hysteresis behavior with no energy dissipation, even when the peak inter-story drifts are 1.50% (the 1st-story) and 1.61% (the 2nd-story) under Northridge with PGA of 1.16 g. It could indicate that the members and connections of BTSF remain elastic with no visible damage, which is appealing for damage control purpose. One inference is that the energy dissipation is predominantly provided by the SWs for the test structure, since BTSF and PTFs remained elastic. After the relatively large drifts in hysteretic cycles, the structure rocked around a balanced position in small cycles and eventually the structure returned to the pre-earthquake position. This suggests that the system has effective self-centering capacity.

4.6. Damage observation

The BTSF, PTFs and floor slabs, including the components and connections, remain elastic (no damage) when the test structure was subjected to base excitation ground motions with different intensity levels. No visible damage such as yielding and cracking were observed in the BTSF, PTFs and floor slabs except for SWs, even when the specimen has been subjected to multiple tests and the peak inter-story drifts of 1.50% and 1.61% happened in Case 1-11 s for the 1st-story and the 2nd-story, respectively. Sample photos taken from the test structure are shown in **Fig. 21**.

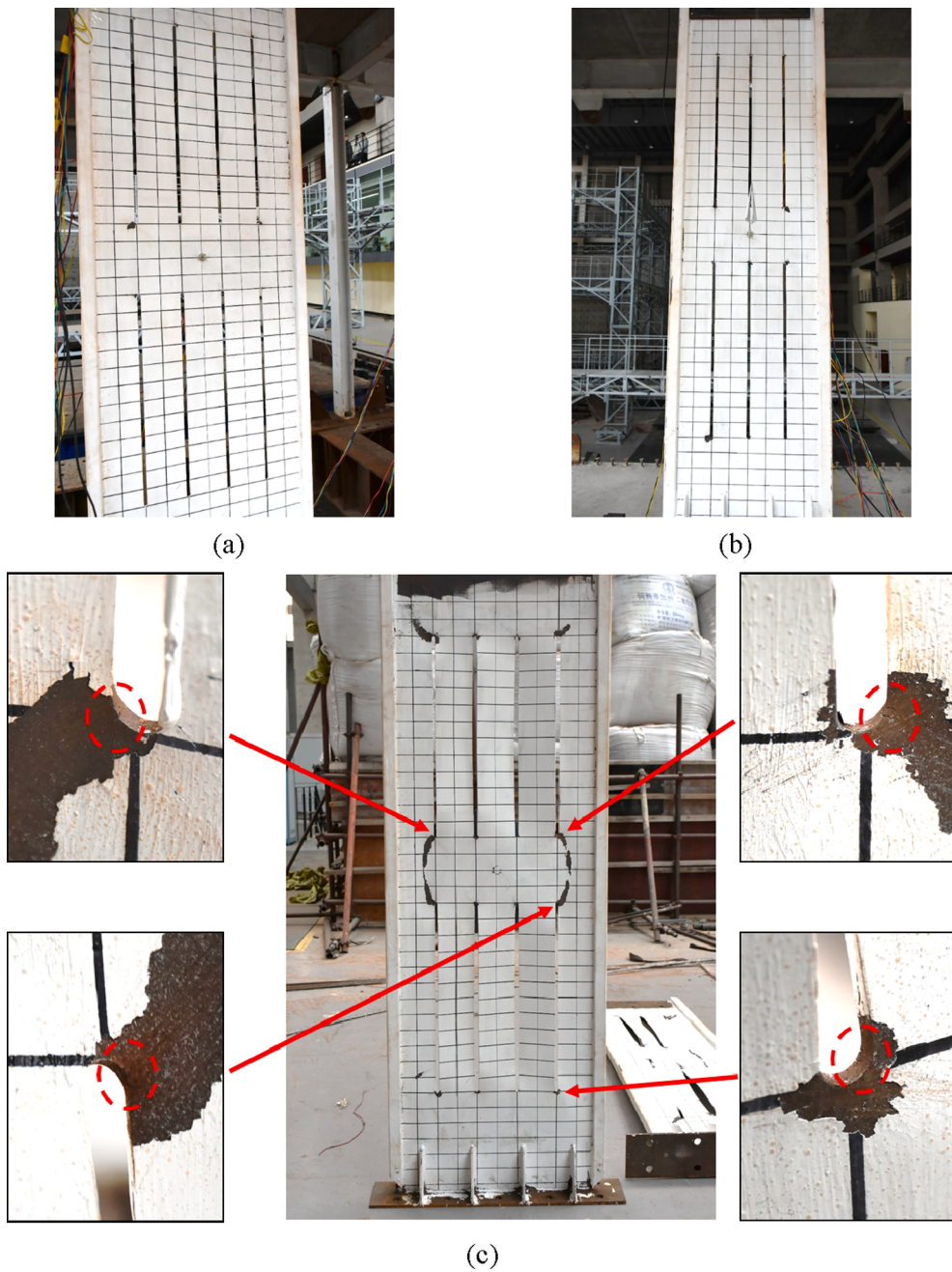


Fig. 22. Photo of SW: (a) 1st-story in Case 1–8; (b) 2nd-story in Case 1–8; (c) 1st-story in Case 1–11 s (removed); (d) 2nd-story in Case 1–11 s (removed).

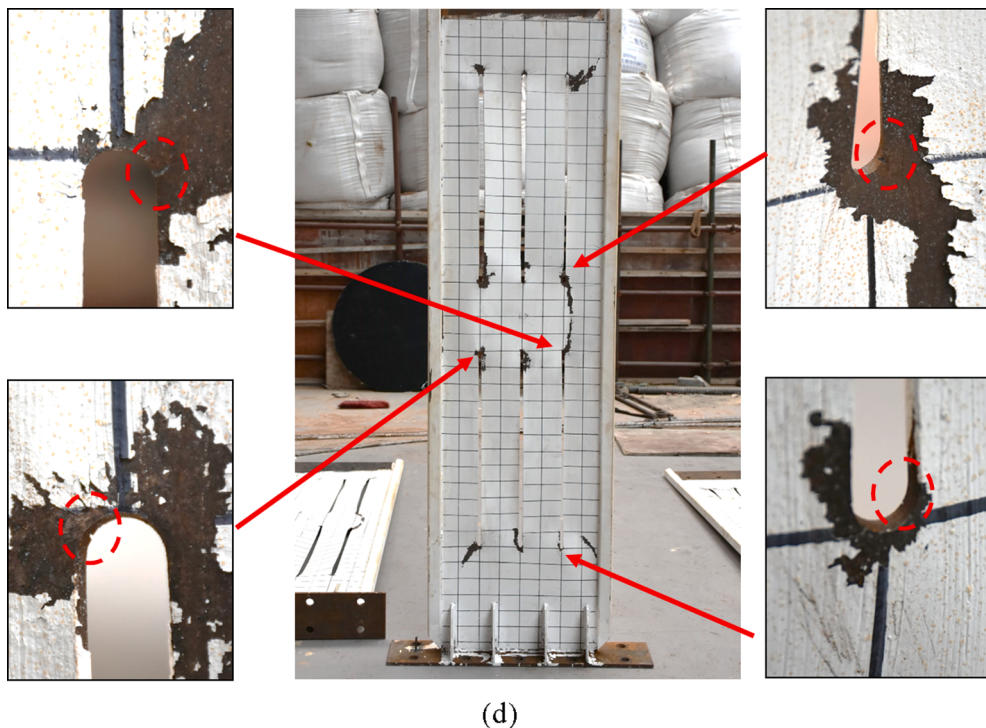
The PT cables force was measured immediately after each test case. The data in Table 6 shows that little prestress has been lost in the tests.

4.7. SW damage evaluation

The SW plays the role of seismic fuse and energy dissipation device in the test structure. In the tests, the SWs remain elastic only in Case 1–2 (Northridge with PGA of 0.11 g) and Case 2–1 (Superstition Hills with PGA of 0.10 g), as shown from measured strain data from local strain gauges around steel slits. For illustration, Northridge earthquake excitation cases (Case 1 series) are discussed here. In Case 1–2, Case 1–4 and Case 1–6, no visible damage was found such as flaking of latex paint due to plastic deformation of SWs. In general, the yielding of SWs begins at the corner of steel slats between slits, and expands to the surrounding corner region of SWs with increasing PGA levels. As illustrated in

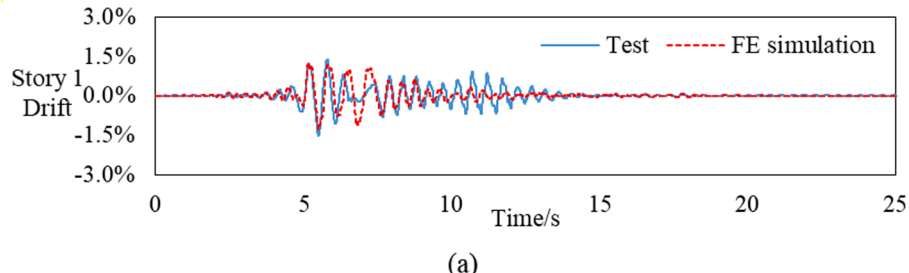
Fig. 22, the photos of SWs taken after Case 1–8 and Case 1–11 s (Northridge with PGA of 0.54 g and 1.16 g) are typical in showing the different damage extents suffered by SWs.

The SWs in Case 1–8 were damaged slightly, as shown in Fig. 23 (a) and (b). The corners of slats between slits yielded (initiating at the end of slits) and the severest damage happened in the outermost slats (judged through the flaking off of white latex paint on the wall). Additionally, the slats are slightly bulgy (out of plane deformation) upon close inspection. As described in Section 4.5, the 1st-story and the 2nd-story sustained an inter-story drift of 1.50% and 1.61% respectively and the SWs dissipated the seismic energy in Case 1–11 s as other components remained elastic without energy dissipation. As shown in Fig. 23 (c) and (d), the plastic zone of the SWs enlarged significantly, and the yielding of the slat corners propagated along nearly 45 degrees line. In the center area of SWs, yield path connected the upper and the bottom slats along

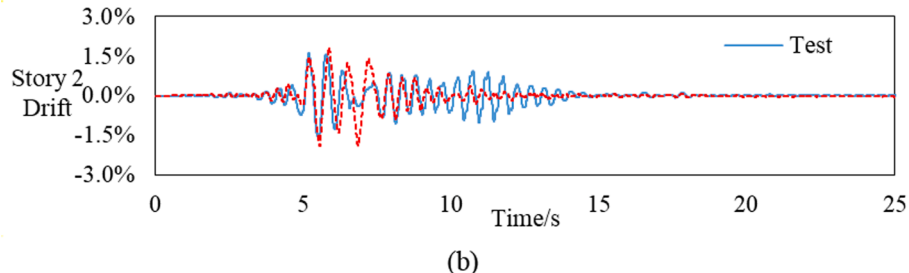


(d)

Fig. 22. (continued).



(a)



(b)

Fig. 23. inter-story drift time history response in FE analysis and test results in Case 1–11 s: (a) 1st-story; (b) 2nd-story.

an arc-like contour. Out-of-plane deformation of the slats also occurred, and slight cracking occurred at the end of slits, as illustrated in Fig. 22(c) and (d). It can be concluded that the SWs experienced large plastic deformation and dissipated seismic energy.

During the shaking table tests, the damaged SWs were replaced once by two crew members after Case 1–11 s. It took a total of 105 min to remove the damaged SWs and install the new SWs (58 min for the 1st-story SW and 47 min for the 2nd-story SW). It is noted that these workers are not highly skilled in doing this as they were not trained before. Replacing the SWs involves removing bolts with wrenches and simple torque wrenches are needed to install the SWs, but otherwise no special tools are required.

4.8. FE modeling validation

Simulation results for Case 1–11 s is presented here to showcase the validity of the finite model. Fig. 23 shows the comparison of inter-story drift time history responses from both FE analysis and experimental test results. Fig. 24 shows the story shear vs. inter-story drift ratio curve and the SW hysteresis curve. In general, a relatively good agreement is observed between results of FE modeling and tests. And it can be concluded that the FE models is validated to simulate the BTSF-SCMP-SW structures with acceptable accuracy.

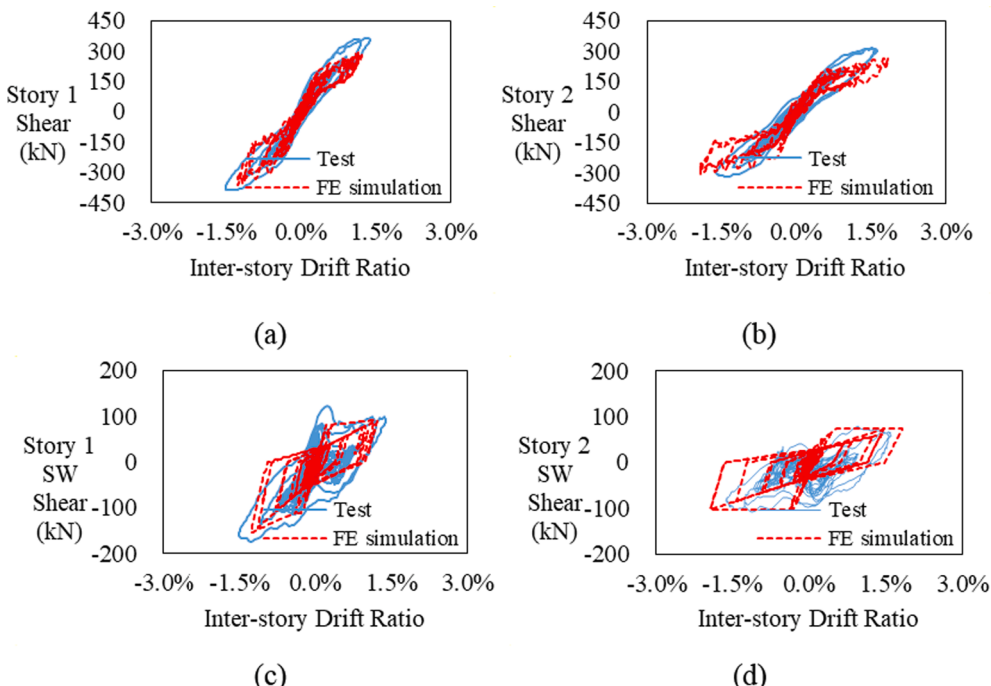


Fig. 24. Hysteresis curves from FE analysis and test results in Case 1–11 s: (a) 1st-story shear; (b) 2nd-story shear; (c) 1st story SW shear; (d) 2nd story SW shear.

5. Conclusion

This paper presents the experimental test results of shaking table tests conducted on a two-story BTSF-SCMP model structure. The seismic performance of the model structure subjected to strong ground motions is investigated, including its self-centering and damage-control behavior. In this system, the BTSF functions as a gravity load carrying frame with negligibly-small lateral stiffness compared with the main seismic-force-resisting system of SCMP comprised of PTF and SW. The PTF provides mainly the re-centering capability through rocking actions at PT connections, while the SW is adopted here as seismic fuse device to dissipate seismic energy. The following conclusions can be drawn from the present study.

- (1) For the selected ground motion records with the PGA value lower than frequent ground motion amplitude, the test structure behaved with linear elastic behavior. After examining measured strain values, it is found that all structural members had remained elastic, including gravity load carrying frame members and SCMP members. The test results also show that the inter-story drift response under frequent ground motions met the limit of 0.4% in the 2010 China Code, CSDB (2010) [38].
- (2) In the cases with ground motion PGA values larger than that of frequent ground motions, the system exhibited a flag-shaped hysteresis curves in measured story shear vs. inter-story drift ratio response, while the PTFs and gravity load carrying frame showed nonlinear elastic behavior and linear elastic response, respectively. The PT connections gap opening was enabled through VBEs' rocking about the HBE flanges. The replaceable seismic fuse devices, SWs, yielded and the slats of SWs twisted out of plane due to buckling.
- (3) The test structure shows satisfactory self-centering and ductile behavior. In Case 1–11 s (Northridge record scaled to PGA of 1.16 g), the peak inter-story drift ratios of the 1st-story and 2nd-story were measured as 1.50% and 1.61%, respectively. After completing the base excitation loading, the test structure was found to return to the pre-loading position with negligibly small residual inter-story drift ratio of 0.019%.

- (4) Damage control, easy repair and resilience behavior of the test structure are also inspected and experimentally validated through shaking table test results. The seismic fuse device - SWs dissipated energy by steel plastic deformation, while remaining structural members and PTF elements in the test structure behaved elastically during the tests. The initial pre-tensioning force of PT cables remain largely unchanged after the tests. The out-of-plane buckling and fracture in the steel slats between the slits in the SWs reduced the lateral force capacity of SWs, and thus due to this reduced force the plastic deformation of SWs did not impede the structure's ability of re-centering. The SW replacement process was recorded, in which only the SWs need to be replaced and each SW replacement took less than one hour for two workers to execute. After repair, the dynamic properties and inter-story drift response were found to be nearly identical to the original test structure.

CRediT authorship contribution statement

Gongling Chu: Conceptualization, Methodology, Software, Formal analysis, Investigation, Data curation, Writing – original draft, Visualization. **Wei Wang:** Conceptualization, Methodology, Supervision, Project administration, Funding acquisition. **Yunfeng Zhang:** Conceptualization, Methodology, Validation, Investigation, Writing – review & editing, Supervision.

Declaration of Competing Interest

The authors declare that they have no known competing financial interests or personal relationships that could have appeared to influence the work reported in this paper.

Acknowledgements

The financial supports from the National Natural Science Foundation of China (NSFC) with Grant Nos. 51778459, 51820105013 and 52078366 are gratefully acknowledged. Supports for this study were also provided by the State Key Laboratory of Disaster Reduction in Civil